Title	Digital computation of the complex linear canonical transform
Author(s)	Liu, Changgeng; Wang, Dayong; Healy, John J.; Hennelly, Bryan M.; Sheridan, John T.; Kim, Myung K.
Publication date	2011-07-01
Publication information	Journal of the Optical Society of America A, 28 (7): 1379-1386
Publisher	Optical Society of America
Link to online version	http://dx.doi.org/10.1364/JOSAA.28.001379
Item record/more information	http://hdl.handle.net/10197/3294
Publisher's statement	This paper was published in Journal of the Optical Society of America. A, Optics and image science and is made available as an electronic reprint with the permission of OSA. The paper can be found at the following URL on the OSA website: http://www.opticsinfobase.org/josaa/abstract.cfm?uri=josaa-28-7-1379. Systematic or multiple reproduction or distribution to multiple locations via electronic or other means is prohibited and is subject to penalties under law.
Publisher's version (DOI)	http://dx.doi.org/10.1364/JOSAA.28.001379

Digital computation of the complex linear canonical transform

Changgeng Liu,[1,2,*] Dayong Wang,[1] John J. Healy,[3,4] Bryan M. Hennelly,[3,4] John T. Sheridan,[5,6,7] and Myung K. Kim[2]

[1]*College of Applied Sciences, Beijing University of Technology, Beijing 100124, China*
[2]*Department of Physics, University of South Florida, Tampa, Florida 33612, USA*
[3]*Department of Computer Science, National University of Ireland, Maynooth, County Kildare, Ireland*
[4]*The Callan Institute, National University of Ireland, Maynooth, County Kildare, Ireland*
[5]*University College Dublin Communications and Optoelectronic Research Centre, University College Dublin, Belfield, Dublin 4, Ireland*
[6]*Science Foundation Ireland (SFI) Strategic Research Cluster in Solar Energy Conversion, University College Dublin, Belfield, Dublin 4, Ireland*
[7]*School of Electrical, Electronic and Mechanical Engineering, College of Engineering, Mathematical and Physical Sciences, University College Dublin, Belfield, Dublin 4, Ireland*
**Corresponding author: changgengliu@mail.usf.edu*

Received January 4, 2011; revised April 16, 2011; accepted May 9, 2011; posted May 11, 2011 (Doc. ID 140544); published June 10, 2011

An efficient algorithm for the accurate computation of the linear canonical transform with complex transform parameters and with complex output variable is presented. Sampling issues are discussed and the requirements for different cases given. Simulations are provided to validate the results.

OCIS codes: 070.4560, 080.2730, 100.2000, 200.2610, 200.3050, 200.4560.

1. INTRODUCTION

The linear canonical transform (LCT) is a class of linear integral transform with three parameters α, β, and γ, which is the general case of many well-known transforms such as the Fourier transform (FT), the fractional Fourier transform (FRT), and the Fresnel transform (FST) [1]. These integral transforms are of great importance in wave propagation problems, because they are the solutions of the wave equation under a variety of circumstances. In optics, the LCT can be used to model paraxial free space propagation and other quadratic phase systems such as thin lenses and graded-index media [2–5]. These systems are modeled as lossless systems using LCTs with real parameters. LCT with complex parameters are also significant because: (i) LCTs with complex parameters can be used to model a class of lossy optical systems, e.g., systems containing Gaussian apodized apertures, in which α, β, and γ are complex and the output domain variable is real [6–9]. (ii) Several transforms of interest are special cases of the LCT with complex parameters, e.g., the Laplace transform (LT), for which $\alpha = \gamma = 0$, and β is a purely imaginary number. Notably, in the LT case, the output variable is complex [1], the generalization of which we consider in this paper. The FT is a special case of the LCT and the LT is a special case of the complex LCT. The well-known relationship between the LT and FT is paralleled in the relationship between the complex and real LCTs. As a consequence, the complex LCT can be calculated for functions whose real LCT does not converge. In this sense, the complex LCT may prove interesting in control theory and other fields. (iii) Sharma, in a recent paper [10] on the fractional LT (a special 1-parameter case of the complex LCT), indicated that "the advantage of the [fractional LT] as compared to the conventional LT lies in providing a free parameter which can be effectively exploited in the filtering and signal separation problems." The complex LCT offers three free parameters for this application. (iv) We speculate that the sampling analysis in Section 2 shows that the complex LCT may be used to suppress the propagation of higher order terms in coherent optical systems which use a spatial light modulator at the input: in a system with complex ABCD parameters, the replicas move off of the real axis, meaning they should be significantly attenuated in the (real) output plane in which a camera captures the wave field. This application requires further study. (v) All LCTs with real parameters are special cases of the more general complex parameters case. As we will see in Section 2, this allows us to analyze certain problems in a fashion not possible if we restrict ourselves to real parameters. See, for example, the sampling analysis of a lens system with a Gaussian aperture, where considering a complex output domain proves fruitful.

In this paper, we discuss the sampling issues of what we will now refer to as the *complex LCT*, i.e., the LCTs with complex parameters and complex argument. The sampling issues for LCTs with real parameters have been discussed in detail in many references [11–19]. When the parameters become complex, however, the output domain variable must in general be dealt with as a complex variable. For some transforms, such as the LT, the output variable is complex, but for most optical systems the output variable is a real spatial variable. We consider a complex output variable primarily for the purposes of sampling analysis. Throughout this paper, the input function is assumed to be a function of a real variable.

Fast algorithms to efficiently compute the LCT with real parameters are widely discussed in the literature based on

the use of decomposition methods or direct methods [20–24]. In some of these algorithms [20,21], the sampling period in the transform domain depends on that employed in the signal domain and on the parameter β. This limits their applicability in computing the LCT with complex parameters. The constraint has subsequently been overcome in the real parameter case [18,19,24], though some modification is still required to calculate the LCT for a complex output variable, and the sampling analyses of those papers do not apply for complex parameters. We also note a recent paper on the fast computation of the complex LCT. The presented method based on the decomposition of complex LCT into three imaginary and three real chirp multiplications and FTs and inverse FTs can efficiently calculate the samples of the function on the real line from an input function on the real line [25].

A natural way to calculate a complex LCT is to decompose its ABCD matrix into a cascade of matrices for which the numerical approximation is well-known. However, for real parameters, this is known to come at the cost of increasing the number of samples required for the calculation [20,26]. In this paper, we present an alternative fast algorithm to compute the complex LCT. As noted, this method has independent sampling periods and total numbers of samples in the signal (input) and transform (output) domain. As we will show, the algorithm computes the samples of the complex LCT along any line of interest in the complex plane. By considering multiple lines, we can synthesize the complex LCT over any region of interest.

The numerical algorithm employed in this paper, i.e., the fast Fourier transform based direct integration (FFT-DI) algorithm, was previously developed in the area of digital holography, where it has been used to provide rapid calculations of wave propagation based on the Rayleigh–Sommerfeld integral and the FST [27–29]. We also note that this algorithm has been employed to efficiently calculate the FRT [30], in which the sampling rate in the output domain depends on that in the input domain. Then, some papers decomposed the LCT into FRT and other operations to efficiently calculate the LCT [22,23]. However, direct application of this algorithm, to perform complex LCT calculations, has never previously been discussed. Issues related to sampling and the resulting synthesis of the full output distribution (as a function of the complex domain variable) are presented. The FFT-DI can be directly applied to computing the two-dimensional FST and provides a novel reconstruction method that can freely set the pixel resolution [28,29].

This paper is organized as follows: in Section 2, sampling and the complex LCT are discussed. In Section 3, a fast algorithm to compute the complex LCT is presented. In Section 4, the validity of the presented algorithm is verified by numerical simulations for some special cases. Finally, some conclusions are given in Section 5.

2. SAMPLING

Assuming $\beta \neq 0$, the LCT of a function $f(x)$ is $g(\xi)$, which can be given by

$$g(\xi) = \sqrt{\beta}\exp(-j\pi/4)\int_{-\infty}^{\infty} f(x)\exp[j\pi(\alpha x^2 - 2\beta x\xi + \gamma\xi^2)]\mathrm{d}x, \tag{1}$$

where $j = (-1)^{1/2}$ and input x is a real variable. In general, α, β, and γ are assumed to be three complex parameters, and ξ to be a complex variable. Let us first define a function which will shortly prove useful,

$$h(\eta) = h(\beta\xi) = \int_{-\infty}^{\infty} f(x)\exp(+j\pi\alpha x^2)\exp(-j2\pi x\beta\xi)\mathrm{d}x, \tag{2}$$

which can be also written as

$$h(\beta\xi) = g(\xi)/\left[\sqrt{\beta}\exp(-j\pi/4)\exp(+j\pi\gamma\xi^2)\right]. \tag{3}$$

The samples of $f(x)$ are $f(m\Delta x)$, in which Δx is the sampling period in the input domain, and m is the sequence number. Let us now explore the expression, $g_d(\xi)$, of the LCT of these samples. We will first examine this function along the line l_0 represented by $\xi = \eta/\beta$, where η is a real variable, as shown in Fig. 1(a), because the convolution theorem can be applied to this region. Then, the result is extended to a region of the complex plane by analytic continuation. Assume ξ_R is the real axis, and ξ_I is the imaginary axis. The complex variable ξ can be written as $\xi_R + j\xi_I$.

On the line l_0, $g_d(\xi)$ is given by

$$\begin{aligned}
g_d(\xi) &= \sqrt{\beta}\exp(-j\pi/4)\exp(+j\pi\gamma\xi^2)\sum_{m=-\infty}^{+\infty} f(m\Delta x)\\
&\quad\times\exp[+j\pi\alpha(m\Delta x)^2]\exp(-j2\pi m\Delta x\beta\xi)\Delta x\\
&= \sqrt{\beta}\exp(-j\pi/4)\exp(+j\pi\gamma\xi^2)\int_{-\infty}^{+\infty} f(x)\exp(+j\pi\alpha x^2)\\
&\quad\times\mathrm{comb}\left(\frac{x}{\Delta x}\right)\exp(-j2\pi x\eta)\mathrm{d}x\\
&= \sqrt{\beta}\exp(-j\pi/4)\exp(+j\pi\gamma\xi^2)[h(\eta)\otimes\Delta x\mathrm{comb}(\Delta x\eta)]\\
&= \sqrt{\beta}\exp(-j\pi/4)\exp(+j\pi\gamma\xi^2)\sum_{m=-\infty}^{\infty} h\left(\eta - \frac{m}{\Delta x}\right)\\
&= \sqrt{\beta}\exp(-j\pi/4)\exp(+j\pi\gamma\xi^2)\sum_{m=-\infty}^{\infty} h\left(\beta\xi - \frac{m}{\Delta x}\right)\\
&= \exp(+j\pi\gamma\xi^2)\sum_{m=-\infty}^{\infty} g\left(\xi - \frac{m}{\beta\Delta x}\right)\\
&\quad/\exp\left[+j\pi\gamma\left(\xi - \frac{m}{\beta\Delta x}\right)^2\right],
\end{aligned} \tag{4}$$

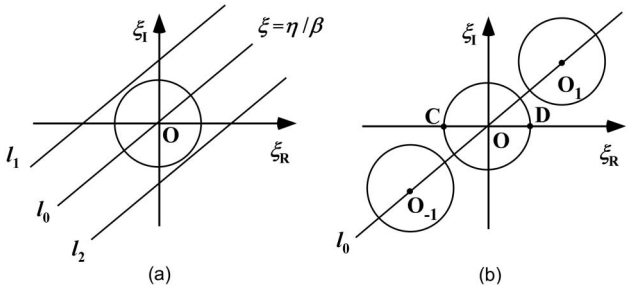

Fig. 1. Illustration for the complex LCT of samples of an input function. ξ_I and ξ_R represent the imaginary and real axis of the complex plane. The radius of the circle is r. (a) $g(\xi)$ is considered to be zero outside the circular area. (b) Shows the periodicity of the shifted replicas in the complex plane.

where $\otimes$ represents convolution operation. We extend Eq. (4) to an area that includes the line l_0. A natural choice for this area is that bounded by two lines which are parallel with l_0. As shown in Fig. 1(a), we choose this area to be that between the lines l_1 and l_2. We assume $g(\xi)$ is an analytic function in this area. Under this assumption, the expression in the last line of Eq. (4) is an analytic function in this area. Because $g_d(\xi)$ identically equals the right term of the first line of Eq. (4) that is a series of analytic functions in the whole complex plane, $g_d(\xi)$ must be an analytic function in the selected area. The theory of the analytic function states that if two functions are analytic in one area and equal along any line in this area, these two functions must be equal over the entire area [31]. Because $g_d(\xi)$ and the expression in the last line of Eq. (4) are both analytic functions in this area and are equal along the line l_0, they must be equal at every point in this area. Thus, if $g(\xi)$ is an analytic function in this area, Eq. (4) must hold in this area.

It can be seen from Eq. (4) that the LCT of the samples of a function consists of periodic shifted replicas of the LCT of this function. Of the three parameters, only β affects the separation of the replicas. The separation of the replicas, or period, is given by

$$P = \frac{1}{\beta \Delta x}. \tag{5}$$

We note that Eq. (5) is consistent with the results for real parameters [11–13,19]. We assume that the function $g(\xi)$ is concentrated in a circular area with radius r, i.e., that it is zero outside this area, as shown in Fig. 1(a). $g_d(\xi)$ can be described by Fig. 1(b), in which the length of the vector OO_1 is given by P in Eq. (5). We require that the support of the replicas not overlap in the region of interest if we are to recover the LCT of the continuous signal from the LCT of the sampled signal. For some cases, ξ is a complex variable, and we must compute the samples of a region of interest centered at the point O_0. For practical optical systems ξ is a real variable, and the region of interest is the line CD along the real axis. For certain parameter values, Eq. (4) may indicate that the replicas are amplified. However, this presents difficulties only if $g(\xi)$ falls off more slowly than the gain increases, which should occur only in impractical systems.

Let us now discuss the selection of the sampling period of the function for the different particular cases of interest.

Case 1. The LT

The one-sided LT is expressed as

$$g(\xi) = \int_0^{+\infty} f(x) \exp(-\xi x) \mathrm{d}x, \tag{6}$$

where $f(x) = 0$ when $x < 0$. Equation. (6) can be rewritten as the LCT of $f(x)$:

$$g(\xi) = \left(\sqrt{\beta} \exp(-j\pi/4) \int_{-\infty}^{\infty} f(x) \exp[j\pi(-2\beta x\xi)] \mathrm{d}x \right) / \left(\sqrt{\beta} \exp(-j\pi/4) \right), \tag{7}$$

where $\beta = -j/(2\pi)$. Equation. (7) indicates that the LT is an LCT with $\alpha = \gamma = 0$, $\beta = -j/(2\pi)$. ξ is a complex variable. In this case, the area of interest is the central circular area in Fig. 1(b). To avoid aliasing (overlapping of the replicas), the sampling period Δx must satisfy

$$\frac{1}{|\beta| \Delta x} \geq 2r. \tag{8}$$

Therefore,

$$\Delta x \leq \frac{1}{2r|\beta|}. \tag{9}$$

Case 2. Lossy optical FT

In Fig. 2, LA represents a limiting aperture which is apodized so that the amplitude transmission function is of the form

$$T = \exp\left(-\frac{x^2}{\sigma^2}\right), \tag{10}$$

where σ is the $1/e$ transmission radius.

The ABCD parameters for this system are determined as follows:

$$M = \begin{pmatrix} 1 & \lambda f \\ 0 & 1 \end{pmatrix} \begin{pmatrix} 1 & 0 \\ j/\pi\sigma^2 & 1 \end{pmatrix} \begin{pmatrix} 1 & 0 \\ -1/\lambda f & 1 \end{pmatrix} \begin{pmatrix} 1 & \lambda f \\ 0 & 1 \end{pmatrix} = \begin{pmatrix} \frac{j\lambda f}{\pi\sigma^2} & \lambda f\left(1 + \frac{j\lambda f}{\pi\sigma^2}\right) \\ \frac{-1}{\lambda f} + \frac{j}{\pi\sigma^2} & \frac{j\lambda f}{\pi\sigma^2} \end{pmatrix}. \tag{11}$$

Hence, $g(\xi)$ at the output plane can be obtained from the input, $f(x)$, using an LCT with ABCD parameters:

$$\alpha = \frac{A}{B} = \frac{1}{\lambda f - j\pi\sigma^2}, \tag{12}$$

$$\beta = \frac{1}{B} = \frac{1}{\lambda f\left(1 + j\frac{\lambda f}{\pi\sigma^2}\right)}, \tag{13}$$

$$\gamma = \frac{D}{B} = \frac{1}{\lambda f - j\pi\sigma^2}. \tag{14}$$

f is the focal length of the lens in Fig. 2, and λ is the wavelength of the light. In this case, β is a complex parameter, and ξ is a real variable (spatial frequency). The region of interest is the section CD, as illustrated in Fig. 1(b). Assume θ is the angle between OO_1 and the real axis. It ranges from 0 to π. θ is given by

$$\theta = \arctan\left(\frac{\pi\sigma^2}{\lambda f}\right). \tag{15}$$

To avoid aliasing the sampling period, Δx must satisfy

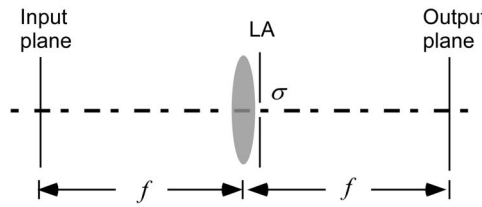

Fig. 2. Optical Fourier transformation system with a Gaussian apodized limiting aperture (LA) of radius σ placed immediately to the right of the transmission lens.

$$\Delta x \le \begin{cases} 1/\left[r|\beta|\sqrt{\cot^2(\theta)+1}\right], & \pi/4 \le \theta \le 3\pi/4 \\ 1/[2r|\beta||\cos(\theta)|], & \text{otherwise} \end{cases}. \quad (16)$$

When θ equals 0 or π, Eq. (16) reduces to Eq. (9).

Case 3. The FST

The FST is employed to model the paraxial free space propagation. The FST is an LCT in which $\alpha = \beta = \gamma = 1/\lambda z$. z is the propagation distance, and λ is the wavelength. In this case, both β and ξ are real valued, and Eq. (16) can be used to determine the sampling period Δx. Evaluation takes place along the real axis, i.e., when $\theta = 0$.

3. DIGITAL COMPUTATION

All existing algorithms can only calculate the LCT along the real output axis [22–25] or a particular line in the complex output plane [20,21], depending on how the output sampling rate is chosen. Therefore, they cannot be employed to perform calculations for Case 1 described above. In this Section, a FFT-DI is presented to calculate the samples of the complex LCT. This method can efficiently compute the samples of the LCT along any line. When it is used in Case 1, the samples of the LCT are calculated separately for many lines, and then the set of individual results are synthesized to approximate the full distribution. In Cases 2 and 3, only the samples along the real axis must be computed.

In practice, only a finite number of input samples of a signal and the resulting output LCT samples are calculated. The input samples of a signal can be given by $\{f(0), \cdots f(m), \cdots f(M-1)\}$, where M denotes the number of samples of the signal and m the sequence number. The resulting output LCT samples can be written by $\{g(0), \cdots g(n), \cdots g(N-1)\}$, where N denotes the number of the resulting output LCT samples and m the sequence number. The relationship between the sample sequence number, m and n, and the coordinates are

$$x = (m - [M/2])\Delta x + x_0, \qquad m \in [0 \quad M-1], \quad (17)$$

$$\xi = (n - [N/2])\Delta\xi + \xi_0, \qquad n \in [0 \quad N-1], \quad (18)$$

where $[-]$ indicates rounding the operand down to the greatest integer less than or equal to it. Δx is the sampling period of the signal. As illustrated in Fig. 3(b), $\Delta\xi$ is the sampling period of the LCT along a line in the complex plane. x_0 and ξ_0 are the coordinates corresponding to the sequence number $[M/2]$ and $[N/2]$, respectively, as illustrated by Figs. 3(a) and 3(b). Since

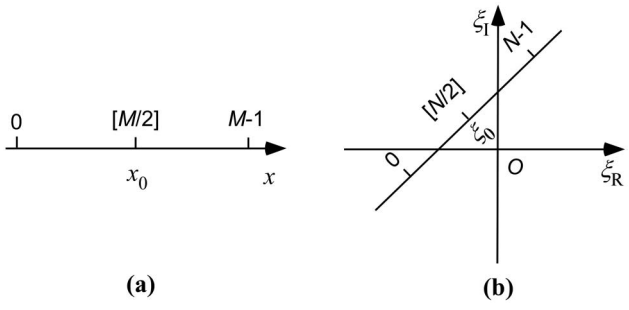

Fig. 3. Relationship between the sequence number and the coordinates.

$\Delta\xi$ and ξ_0 can be set freely, the LCT along any line in the complex plane can be obtained.

Substituting Eqs (17) and (18) into Eq. (1), the discrete form of the LCT is given by

$$g(n) = c(n)\sum_{m=0}^{M-1} a(m)b(n-m), \quad (19)$$

where $n \in [0, N-1]$, $m \in [0, M-1]$,

$$\begin{aligned} c(n) = {} & \Delta x\sqrt{\beta}\exp(-j\pi/4)\exp\left\{+j\pi\left[\alpha\left(\left[\frac{M}{2}\right]\Delta x + x_0\right)^2\right.\right. \\ & \left.\left. + \gamma\left(\left[\frac{N}{2}\right]\Delta\xi + \xi_0\right)^2\right]\right\} \\ & \times \exp\left\{-j2\beta\pi\left(x_0\xi_0 + \left[\frac{M}{2}\right]\left[\frac{N}{2}\right]\Delta x\Delta\xi - \left[\frac{M}{2}\right]\xi_0\Delta x\right.\right. \\ & \left.\left. - \left[\frac{N}{2}\right]x_0\Delta\xi\right)\right\} \times \exp\{+j\pi n^2(\gamma\Delta\xi^2 - \beta\Delta x\Delta\xi)\} \\ & \times \exp\left\{+j2\pi n\left[\gamma\Delta\xi\left(\xi_0 - \left[\frac{N}{2}\right]\Delta\xi\right) - \beta(x_0\Delta\xi\right.\right. \\ & \left.\left. - \left[\frac{M}{2}\right]\Delta x\Delta\xi)\right]\right\}, \end{aligned} \quad (20)$$

$$\begin{aligned} a(m) = {} & f(m)\exp\{+j\pi m^2(\alpha\Delta x^2 - \beta\Delta x\Delta\xi)\} \\ & \times \exp\left\{+j2\pi m\left[\alpha\Delta x\left(x_0 - \left[\frac{M}{2}\right]\Delta x\right)\right.\right. \\ & \left.\left. - \beta\left(\xi_0\Delta x - \left[\frac{N}{2}\right]\Delta x\Delta\xi\right)\right]\right\}, \end{aligned} \quad (21)$$

$$b(m) = \exp(+j\pi\beta m^2\Delta x\Delta\xi). \quad (22)$$

Equation (19) is a discrete linear convolution that can be efficiently computed by converting it into a cyclical convolution and then employing the fast Fourier transform (FFT) algorithm. A flow chart showing the specific computational operations is given in Fig. 4.

Because the FFT-DI is a fast computational method for direct integration (DI) of the LCT, the only error source arises

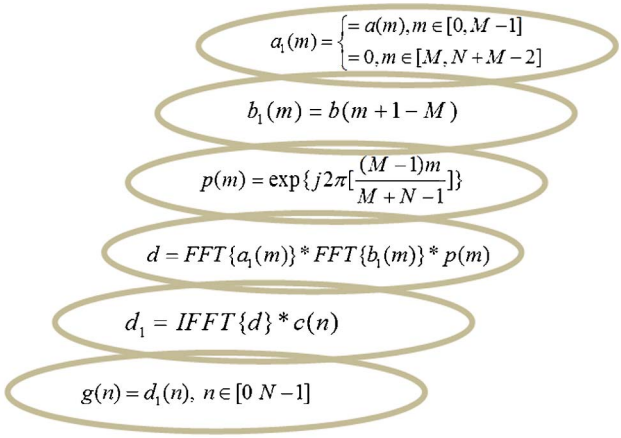

Fig. 4. (Color online) Flow chart of the FFT-DI. The operation * indicates an inner product of the two data vectors, i.e., their entry-wise product.

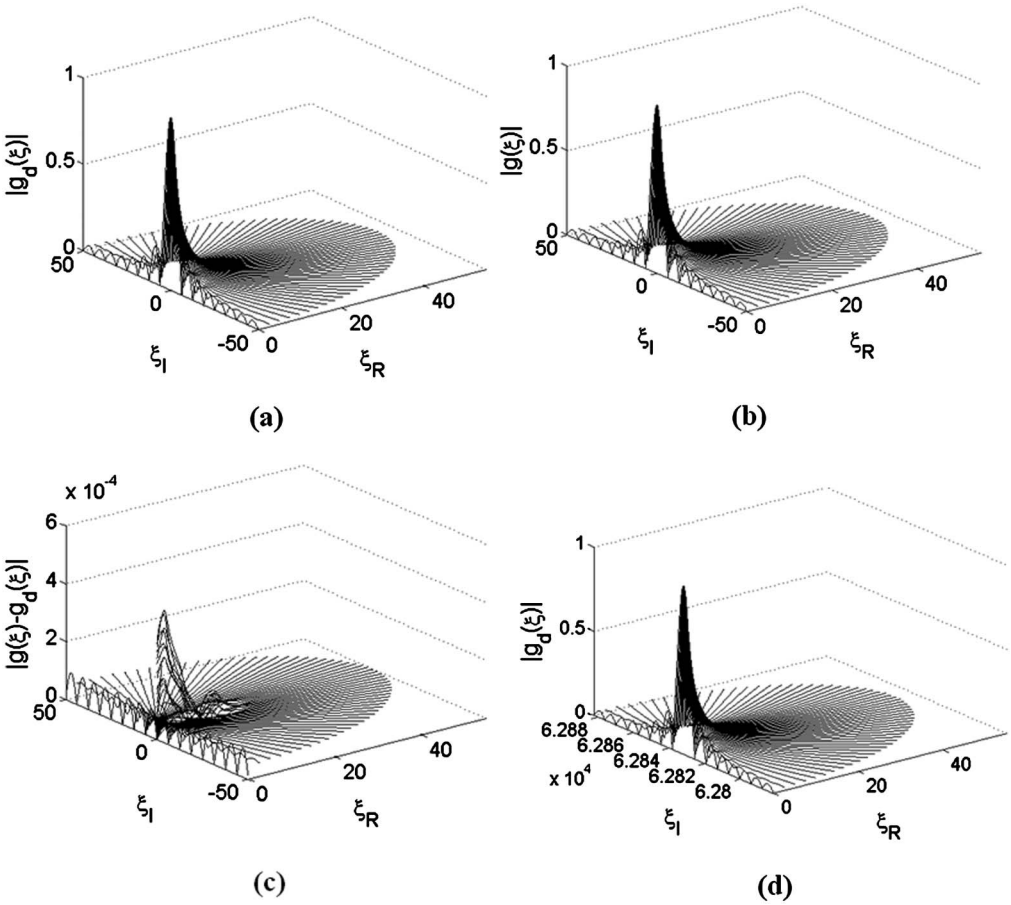

Fig. 5. Results of simulations using the different methods: (a) the zero order by the FFT-DI, (b) the analytical formula, (c) the difference between the results presented in (a) and (b). (d) The first replica by the FFT-DI.

from the use of the FFT when approximating the discrete Fourier transform (DFT). The numerical complexity of this algorithm can be estimated as

$$O[(M+N)\log(M+N)], \tag{23}$$

and the operation time is dominated by three calls to the FFT algorithm. From Eq. (23), it follows that the complexity of this algorithm is comparable to the existing algorithms for computing the LCT with real parameters and a real variable, and the existing algorithm for computing the LCT with complex parameters and a real variable [25].

4. SIMULATIONS AND DISCUSSIONS

In this Section, we will employ the FFT-DI to compute examples for the three cases discussed in Section 2.

Case 1. The LT

$\mathrm{rect}(x-1/2)$, whose LT is an analytic function, is substituted it into Eq. (6) or (7):

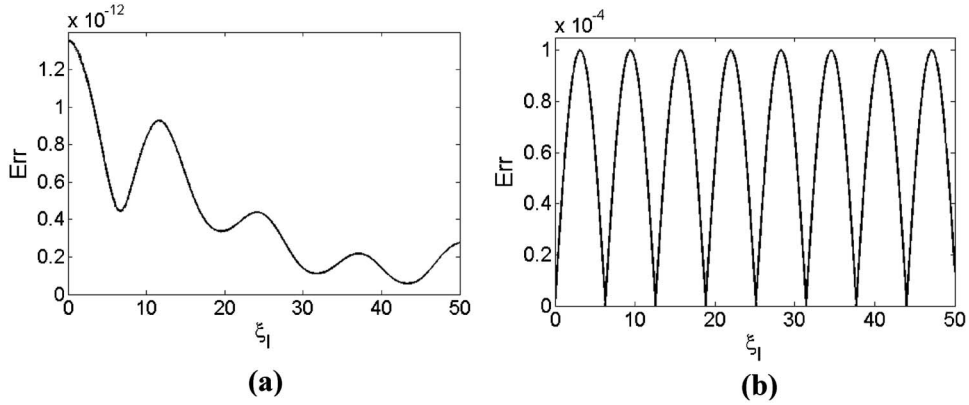

Fig. 6. Deviations between the different methods calculated for results along the imaginary axis of the complex plane. (a) The differences between the FFT-DI and the DI results. (b) The deviation of the FFT-DI from the analytical formula.

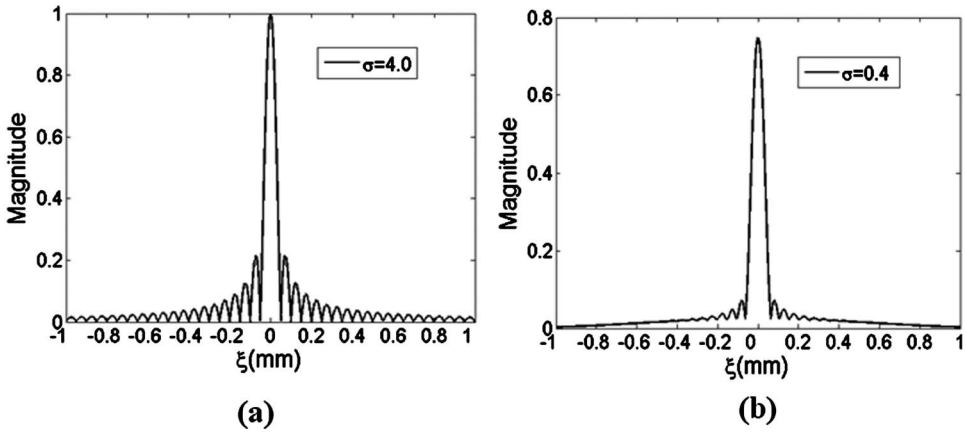

Fig. 7. Outputs of an Fourier transformation system with lossy Gaussian apodized apertures of different widths. (a) $\sigma = 4.0\,\mathrm{mm}$ and (b) $\sigma = 0.4\,\mathrm{mm}$.

$$g(\xi) = \int_0^1 \exp(-\xi x)\mathrm{d}x = \begin{cases} [1 - \exp(-\xi)]/\xi, & \xi \neq 0 \\ 1, & \xi = 0 \end{cases}. \quad (24)$$

This is analytic in the whole complex plane, and thus Eq. (4) holds for this test function. The period of this function is $+j2\pi/\Delta x$, which indicates that replicas extend along the imaginary axis. However, Eq. (24) does not converge on the whole complex plane, so we restrict the area of interest to the semiplane for which $\mathrm{Re}(\xi) \geq 0$. In this area, Eq. (24) converges. Consider an arbitrary line through the origin, $\xi = x/c$, where x is a real variable, and c is some complex number of unit magnitude which characterizes the line. Along this line, Eq. (24) has the form

$$g(\xi) = g(cx) = \frac{c}{x}[1 - \exp(-x/c)]. \quad (25)$$

Thus, the function can be written as a constant multiplied by a linear decay multiplied by an oscillatory component. From Eq. (25), we can make the assumption that there is a semicircular area, outside of which $g(\xi) \approx 0$. Within this semicircular area, the following inequality holds

$$|g(\xi)| \leq k|g(\xi)|_{\max}, \quad (26)$$

where k is a real number. Equation. (26) is used to estimate the cutoff radius r. When $k = 10^{-4}$, it is estimated that $r \approx 2 \times 10^4$. In this case, Eq. (8) indicates that the sampling value chosen, Δx, should be not larger than $1/6366$ to avoid aliasing. Since the FFT-DI efficiently computes the samples of the LCT along any line passing through the origin, we calculate sample values along many such lines, and then synthesize these results to generate the complete output data set within the semicircular area, see Fig. 5.

In Fig. 5(a), the resulting set of $g_d(\xi)$ values calculated by the FFT-DI are plotted over the appropriate semicircular area in the complex plane. The samples lie along 61 lines of equal angular separation of 3°. Each line is calculated separately and the 61 sets of data are then combined to produce the whole distribution. The sampling period chosen is $\Delta x = 10^{-4}$, which is less than $1/6366$. Then, for comparison, the analytical expression in Eq. (24) is plotted in Fig. 5(b). The difference between these two results is given in Fig. 5(c). To prove the validity of Eq. (4), the first replica is shown in Fig. 5(d).

If the sampling period is further reduced, the effects of aliasing decrease. Compared with the DI method, deviation can arise in the FFT-DI because of errors introduced when using the FFT to approximate the DFT. This deviation is, however, negligible when compared to the differences between the results of the FFT-DI and the analytical formula. The relative sizes of these two types of error are shown in Fig. 6. In Fig. 6(a), the very small deviation between results produced using the FFT-DI and the DI along the imaginary axis are presented, while in Fig. 6(b) the difference between the equivalent results produced using the FFT-DI and those generated

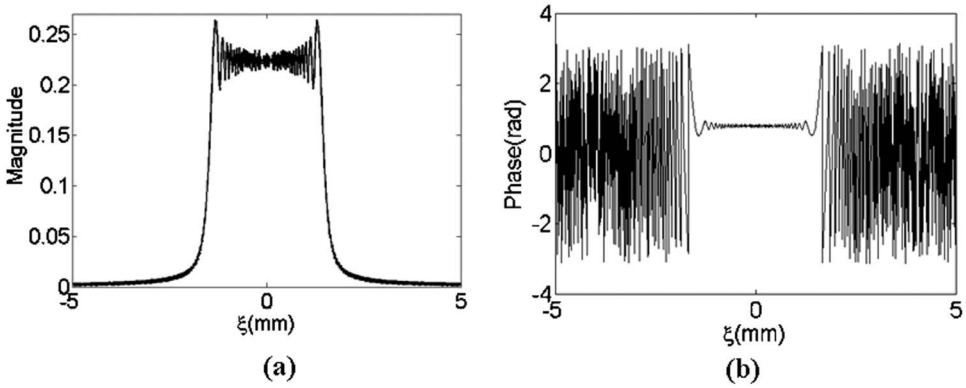

Fig. 8. Discrete FST results calculated using the FFT-DI with $\alpha = \gamma = 1/\lambda d$. (a) The magnitude and (b) the corresponding phase predictions.

using the analytical formula are given. The differences indicated in Fig. 6(b) are more regular than those in Fig. 6(a) and are typically several orders of magnitude larger.

Case 2. Lossy optical FT

Next, we apply the FFT-DI to compute the output of the lossy optical Fourier transformation system shown in Fig. 2. We arbitrarily chose $\lambda = 500\,\text{nm}$ and $f = 100\,\text{mm}$. The input function is a rectangular function equal to 1 in the range -0.5 to $+0.5\,\text{mm}$ and to 0 everywhere else. Three thousand samples are taken over this range to avoid aliasing noise. Figure 7(a) shows the result for an apodized Gaussian lossy aperture of the radius $\sigma = 4.0\,\text{mm}$. In this case, the loss of light is very small, i.e., little light is obstructed or absorbed by the aperture. Therefore, the predicted output closely approximates the ideal lossless FT of the rectangular input function, which can be expressed as $\text{sinc}(20\xi)$.

When, however, σ is reduced to $0.4\,\text{mm}$, and significantly more light is affected by the attenuating aperture, the central peak and sidelobes of the output are suppressed in size, as shown in Fig. 7(b).

Case 3. The FST

Finally, we apply the FFT-DI to calculate the discrete FST for $\lambda = 500\,\text{nm}$ and $d = 100\,\text{mm}$. The input function used is again a rectangular function equal to 1 in the range -1.5 to $+1.5\,\text{mm}$ and to 0 everywhere else. One thousand and twenty-four samples over this range are necessary to avoid aliasing effects. In this case, $\alpha = \gamma = \beta = 1/\lambda d$. The resulting magnitude and phase predictions are given in Fig. 8.

We note as a further motivation for performing this research that the FFT-DI can be directly applied to compute the two-dimensional FST, providing a novel reconstruction method that can be used to flexibly set the pixel resolution. This application has previously been discussed in [28,29].

5. CONCLUSIONS

In this paper, a sampling theory and fast algorithm for the numerical approximation of complex LCTs, i.e., LCTs with complex parameters and a complex output variable, have been developed. Supporting simulations have been presented.

Given a function, sampled with period Δx, the LCT of this function is periodic in the complex output plane. The periodicity occurs along a line given by x/β, where x is a real variable. It has period $P = 1/(\beta\Delta x)$. This result is consistent with the sampling theorem for LCTs with real variables: real β implies that periodicity occurs along the real axis of the output domain. The sampling requirements for a number of special cases have been determined. We note that for complex values of β, it is possible for no replicas to appear on the real axis, which suggests applications in digital holography, where removal of these replicas may be a priority.

The FFT-DI algorithm, an algorithm which has been previously used in the numerical approximation of the Rayleigh–Sommerfeld integral and the FST [27–29], is adapted to compute the LCT for some area of the complex plane. For N input samples and M output samples, it does this in order $(N + M)\log(N + M)$ time. Letting $N = M$, this algorithm has $O(N \log N)$ complexity, comparable to existing LCT algorithms [20–24]. However, existing algorithms can only calculate the LCT along the real output axis [22–24] or a particular line in the complex output plane [20,21], depending on how the output sampling rate is chosen. The FFT-DI algorithm can be used to rapidly calculate the samples of the LCT along any line in the complex plane. The individual set of results along each line can then be combined to synthesize the full distribution over this area. Furthermore, existing LCT algorithms restrict $N = M$ unless interpolation and/or decimation algorithms are used. Thus, the FFT-DI algorithm is also of interest for the simulation of LCTs with real parameters.

Results calculated using the FFT-DI, applied to three different cases have been presented and compared to the equivalent analytic result. Based on the results of the simulations, it is claimed that the FFT-DI has proven itself to be an accurate and efficient algorithm for computing the complex LCT. The algorithm should prove useful in a number of applications, including the study of systems with apertures, propagation in scattering media, and digital holography.

ACKNOWLEDGMENTS

This research is supported in part by the Science Foundation of Education Commission of Beijing under grant KZ20091 0005001 and by the Funding Project for Academic Human Resources Development in Institutions of Higher Learning Under the Jurisdiction of Beijing Municipality. JJH, BMH, and JTS acknowledge the support of the Science Foundation Ireland under the National Development Plan. BMH acknowledges the support of the European Community's Seventh Framework Programme FP7/2007–2013 under grant 216105 "Real 3D".

REFERENCES

1. K. B. Wolf, *Integral Transforms in Science and Engineering* (Plenum, 1979).
2. S. Abe and J. T. Sheridan, "Optical operations on wave functions as the Abelian subgroups of the special affine Fourier transformation," Opt. Lett. **19**, 1801–1803 (1994).
3. S. A. Collins, "Lens-system diffraction integral written in terms of matrix optics," J. Opt. Soc. Am. **60**, 1168–1177 (1970).
4. M. J. Bastiaans, "Wigner distribution function and its application to first-order optics," J. Opt. Soc. Am. **69**, 1710–1716 (1979).
5. H. O. Bartelt, K.-H. Brenner, and A. W. Lohmann, "The Wigner distribution function and its optical production," Opt. Commun. **32**, 32–38 (1980).
6. H. T. Yura and S. G. Hanson, "Optical beam wave propagation through complex optical systems," J. Opt. Soc. Am. A **4**, 1931–1948 (1987).
7. H. T. Yura, S. G. Hanson, and T. P. Grum, "Speckle: statistics and interferometric decorrelation effects in complex ABCD optical systems," J. Opt. Soc. Am. A **10**, 316–323 (1993).
8. H. T. Yura, B. Rose, and S. G. Hanson, "Dynamic laser speckle in complex ABCD optical systems," J. Opt. Soc. Am. A **15**, 1160–1166 (1998).
9. P. A. Bélanger, A. Hardy, and A. E. Siegman, "Resonant modes of optical cavities with phase-conjugate mirrors," Appl. Opt. **19**, 602–609 (1980).
10. K. K. Sharma, "Fractional Laplace transform," Signal, Image and Video Processing **4**, 377–379 (2009).
11. B. Deng, R. Tao, and Y. Wang, "Convolution theorems for the linear canonical transform and their applications," Science in China Ser. F **49**, 592–603 (2006).
12. B.-Z. Li, R. Tao, and Y. Wang, "New sampling formulae related to linear canonical transform," Signal Process. **87**, 983–990 (2007).
13. J.-J. Ding, "Research of fractional Fourier transform and linear canonical transform," Ph.D. dissertation (National Taiwan University, 2001).
14. J. Zhao, R. Tao, and Y. Wang, "Sampling rate conversion for linear canonical transform," Signal Process. **88**, 2825–2832 (2008).
15. F. Gori, "Fresnel transform and sampling theorem," Opt. Commun. **39**, 293–297 (1981).

16. J. J. Healy and J. T. Sheridan, "Sampling and discretization of the linear canonical transform," Signal Process. **89**, 641–648 (2009).
17. J. J. Healy, B. M. Hennelly, and J. T. Sheridan, "An additional sampling criterion for the linear canonical transform," Opt. Lett. **33**, 2599–2601 (2008).
18. F. Oktem and H. M. Ozaktas, "Exact relation between continuous and discrete linear canonical transforms," IEEE Signal Process. Lett. **16**, 727–730 (2009).
19. A. Stern, "Sampling of linear canonical transformed signals," Signal Process. **86**, 1421–1425 (2006).
20. J. J. Healy and J. T. Sheridan, "Fast linear canonical transforms," J. Opt. Soc. Am. A **27**, 21–30 (2010).
21. B. M. Hennelly and J. T. Sheridan, "Fast numerical algorithm for the linear canonical transform," J. Opt. Soc. Am. A **22**, 928–937 (2005).
22. A. Koç, H. M. Ozaktas, C. Candan, and M. A. Kutay, "Digital computation of linear canonical transforms," IEEE Trans. Signal Process. **56**, 2383–2394 (2008).
23. H. M. Ozaktas, A. Koç, I. Sari, and M. A. Kutay, "Efficient computation of quadratic-phase integrals in optics," Opt Lett. **31**, 35–37 (2006).
24. J. J. Healy and J. T. Sheridan, "Reevaluation of the direct method of calculating Fresnel and other linear canonical transforms," Opt. Lett. **35**, 947–949 (2010).
25. A. Koç, H. M. Ozaktas, and L. Hesselink, "Fast and accurate algorithm for the computation of complex linear canonical transforms," J. Opt. Soc. Am. A **27**, 1896–1908 (2010).
26. J. J. Healy and J. T. Sheridan, "Space–bandwidth ratio as a means of choosing between Fresnel and other linear canonical transform algorithms," J. Opt. Soc. Am. A **28**, 786–790 (2011).
27. F. Shen and A. Wang, "Fast-Fourier-transform based numerical integration method for the Rayleigh-Sommerfeld diffraction formula," Appl. Opt. **45**, 1102–1110 (2006).
28. F. Jia, "Study on the principle and applications of digital holography," Master's dissertation (Northwest University, 2008).
29. C. Liu, D. Wang, and Y. Zhang, "Comparison and verification of numerical reconstruction methods in digital holography," Opt. Eng. **48**, 105802 (2009).
30. H. M. Ozaktas, O. Arikan, M. A. Kutay, and G. Bozdagi, "Digital computation of the fractional Fourier transform," IEEE Trans. Signal Process. **44**, 2141–2150 (1996).
31. J. W. Brown and R. V. Churchill, *Complex Variables and Applications* (McGraw- Hill, 2004).